quoted therein.
[8]J. H. Stamper, J. Chem. Phys. 43, 759 (1965).
[9]G. Copley, B. P. Kibble, and L. Krause, Phys. Rev. 163, 34 (1967).
[10]J. N. Dodd, E. Enemark, and A. Gallagher, J. Chem. Phys. 50, 4838 (1969).
[11]J. S. Deech, J. Pitre, and L. Krause, Can. J. Phys. 49, 1976 (1971).
[12]V. Kempter, B. Kübler, and W. Mecklenbrauch, J. Phys. B 7, 2375 (1974).
[13]P. Hannaford and R. M. Lowe, J. Phys. B 9, 2595 (1976).
[14]J. V. Sullivan and A. Walsh, Spectrochim. Acta 21, 727 (1965).
[15]E. E. Gibbs and P. Hannaford, J. Phys. B 9, L225 (1976).
[16]R. M. Lowe, Spectrochim. Acta, Part B 26, 201 (1971).
[17]J. A. Kernahan, E. H. Pinnington, A. E. Livingston, and D. J. G. Irwin, Phys. Scr. 12, 319 (1975).

Rapid Thermal Transport from Turbulent Skin Layer to Plasma Core in a Toroidal Experiment

Y. Nishida,* A. Hirose, and H. M. Skarsgard
Department of Physics, University of Saskatchewan, Saskatoon, Canada, S7N 0W0
(Received 9 December 1976)

Anomalously rapid thermal transport from a skin layer to the plasma core has been observed in a toroidal turbulent heating experiment. The thermal transport rate is approximately two orders of magnitude faster than the classical rate based on the anomalous electron collision frequency.

Skin effects in toroidal turbulent heating experiments have been reported by several groups.[1-3] However, little is known of the transport of energy created in the skin layer, whether it is lost to the vacuum wall or it penetrates into the plasma core. In proposed schemes for turbulently heating a large toroidal plasma,[4] such as a reactor-size tokamak, one crucial assumption is that the thermal energy deposited in the skin layer is rapidly transported toward the plasma core. Otherwise, the electron temperature in the skin layer would become undesirably high, prematurely quenching current-driven instabilities. Although the assumption is based on some experimental facts previously reported, these were obtained in plasmas with a skin layer artificially created by ring electrodes[5] or a nonuniform electric field.[6]

In this Letter, we report experimental observations of rapid thermal transport from a genuine current skin layer toward the plasma core during a time interval when energy loss is still unimportant. The experiment is performed in a toroidal device described previously.[6,7] The mode III operation, or tokamak mode, is employed. A helium plasma with an electron density $(5-10)\times10^{13}$ cm^{-3} is prepared by rf preionizer and preheater pulses in a toroidal magnetic field of 3 kG. A toroidal electric field with a quarter period of 2.0 μs is inductively applied by discharging a 2.5 μF, 50 kV capacitor. Diagnostic methods include a 76-GHz microwave interferometer[8] for the electron density measurements, a small movable magnetic probe for measuring the local magnetic field (both poloidal and toroidal components), a small Rogowsky coil for direct measurement of the local current density, and a diamagnetic Rogowsky coil wound around the feeder cable to the toroidal magnetic field coils. The local magnetic field measurements yield a plasma current-density profile and a plasma pressure profile, and the diamagnetic Rogowsky coil measures the average plasma pressure. The total energy input into the plasma can be calculated from the total plasma current (measured by a Rogowsky coil) and the output voltage from a one-turn loop corrected for the plasma inductance.[9]

Figure 1 shows typical examples of the radial distribution of the poloidal magnetic field B_p and the change (increase) in the toroidal magnetic field ΔB_φ, observed at different times in the discharge, for $n_e\simeq1\times10^{14}$ cm^{-3}. [As shown later, in Fig. 4, β_p (poloidal beta) never exceeds unity and the plasma stays paramagnetic—hence the observed increase in the toroidal magnetic field.] The toroidal current density j_z can be calculated from $j_z\simeq\partial(rB_p)/r\partial r$ and is in agreement with direct measurements made with use of the small Rogowsky coil (Fig. 2). It is clearly seen from Figs. 1 or 2 that the plasma current is limited to a skin layer until about 1.5 μs after applying the main heating field. During this time interval, the distribution of the current layer is stable. After 1.5 μs the skin current penetrates into the column center within 0.3–0.5 μs.

The profile of the plasma pressure $P_\perp=n(T_e+T_i)$ over the cross section of the plasma column

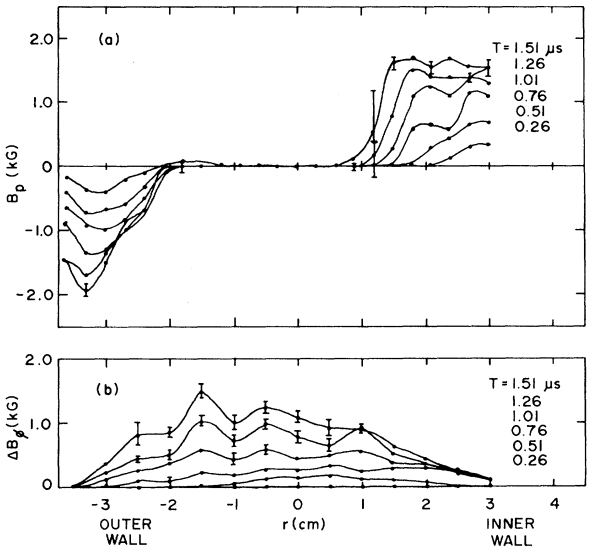

FIG. 1. Time evolution of (a) the poloidal magnetic field strength and (b) the change of toroidal magnetic field strength as a function of the radial position. (b) shows that the plasma is paramagnetic.

can be determined from the field distribution shown in Fig. 1, provided that the plasma is in equilibrium. In the case of axial symmetry, $P_\perp$ is given by[5,10]

$$\frac{\partial P}{\partial r} = -\frac{1}{4\pi}\left[\frac{B_p}{r}\frac{\partial}{\partial r}(rB_p) + B_\varphi \frac{\partial B_\varphi}{\partial r}\right]. \quad (1)$$

The toroidal correction to Eq. (1) is negligibly small. We have numerically integrated Eq. (1) for the observed magnetic-field profiles shown in Fig. 1. The results are shown in Fig. 2 as solid lines. At an earlier time ($t \lesssim 0.26$ μs) the plasma pressure is determined by the preheater, and is almost flat over the entire region. When the main heating becomes effective, the pressure first increases in the skin current region. However, the pressure profile rapidly becomes flattened, within 0.3–0.5 μs, indicating an extremely fast thermal transport. A very nonuniform pressure profile, peaked in the skin layer, would have been observed if there were no energy escape from the skin layer, since energy is continuously deposited there. Figure 3 shows the results for a lower density ($n_e \simeq 7\times10^{13}$ cm^{-3}). Flat pressure profiles are again predominant.

The effective electric field strength and the total plasma current along the toroidal direction are shown in Fig. 4(a). The conductivity σ calculated from the electric field and the current density is shown in Fig. 4(b). The conductivity is at least two orders of magnitude smaller than that

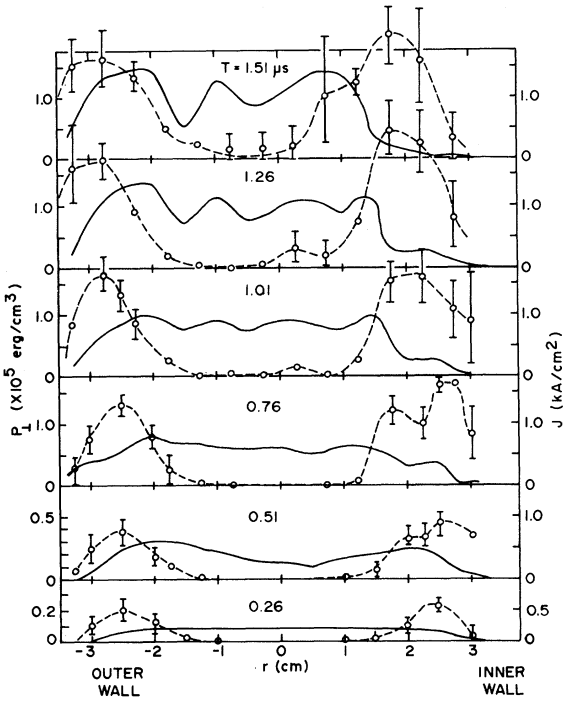

FIG. 2. Time evolution of the profile of plasma pressure (solid line) and current density (broken line). $B_\varphi = 2.9$ kG; $n_e \simeq 1\times10^{14}$ cm^{-3}.

based on classical electron-ion collision.[11] The time evolution of the electron temperature T_e shown in Fig. 4(b) is obtained from the plasma pressure in Fig. 2, neglecting the ion temperature T_i ($\lesssim 50$ eV, as obtained spectroscopically

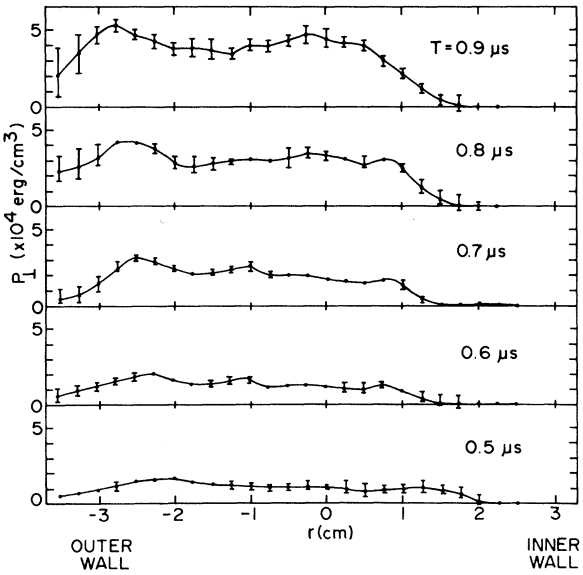

FIG. 3. Time evolution of the profile of plasma pressure for $n_e \simeq 7\times10^{13}$ cm^{-3}, $B_\varphi = 2.95$ kG.

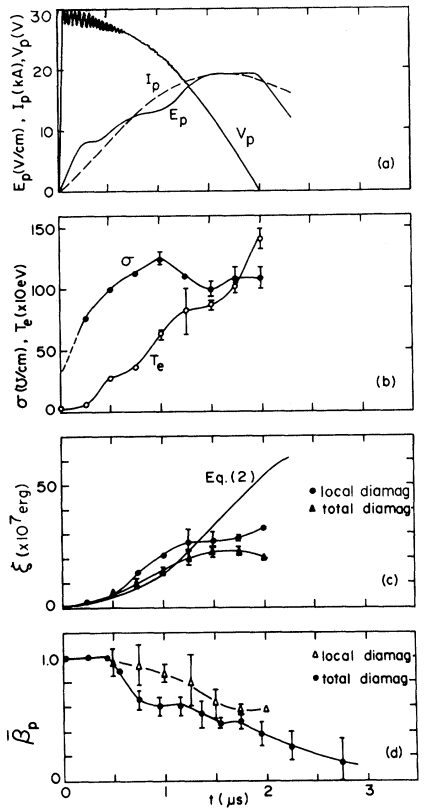

FIG. 4. (a) The toroidal electric field strength E_p, the total plasma current I_p, and the voltage V_p as a function of time. (b) Time evolution of the plasma conductivity σ in the skin layer and the electron temperature T_e. (c) The energy deposited in the plasma (dashed line) and the energy content in the plasma (closed circle) obtained from local pressure measurement, and (closed triangle) from the total diamagnetic signal. (d) Average poloidal β obtained from local plasma pressure (open triangles) and from total diamagnetic signal (closed circles). $n_e \simeq 1\times10^{14}$ cm^{-3}; $B_\varphi = 2.9$ kG.

by monitoring the He II 4686-Å line). The heating rate is about 7.3×10^8 eV/sec.

The total plasma energy is estimated from three independent sets of data. First, the total energy deposited in the plasma can be calculated from

$$\epsilon_1 = 2\pi R\int_0^t I_p(t')E_p(t')dt', \tag{2}$$

where R is the major radius. The results are shown in Fig. 4(c) as a solid line. Second, the integration of the local plasma pressure yields

$$\epsilon_2 = \tfrac{3}{2}V[\,2\int_0^a P(r)\pi r\,dr/\pi a^2] \equiv \tfrac{3}{2}V\bar{P}_\perp, \tag{3}$$

where V is the total plasma volume and a is the minor radius. Third, the measurement of the total diamagnetic effect gives

$$\epsilon_3 = \tfrac{3}{2}\bar{\beta}_p\frac{[\,B_p(a)]^2}{8\pi}V, \tag{4}$$

where $\bar{\beta}_p$ is the average poloidal β factor shown in Fig. 4(d). The observed plasma energy (ϵ_2, ϵ_3) shows reasonable agreement with the energy input (ϵ_1) until about 1.5 μs, after which they deviate because of energy loss.

The observed skin-current profiles can be explained in terms of semiclassical diffusion[12] based on the field penetration associated with the anomalous collision frequency. The electron drift velocity in the skin layer is $(3.8-13)\times10^7$ cm/sec, which is an order of magnitude larger than the ion sound velocity C_s of $(3.4-14.2)\times10^6$ cm/sec. Since $T_e \gg T_i$, the skin layer is subject to the ion acoustic instability. That the observed energy transport is mainly due to electron thermal conduction, and not electron convection or diffusion, is evident from the current profiles shown in Figs. 1 and 2. The skin layer stays at the original location for at least 1.5 μs, and the energy transport is completed well before 1.5 μs. If particle convection were responsible, rapid penetration of the current would have been observed.

The speed of the thermal transport, estimated from the ratio of the plasma radius to the pressure flattening time, is of the order of the ion acoustic speed, which is about two orders of magnitude larger than the classical rate $v_T^2K_T\nu/\omega_{ce}^2$, where v_T is the electron thermal speed, K_T ($\sim 1/a$) is the temperature-scale coefficient, ν is the anomalous collision frequency, and ω_{ce} is the electron cyclotron frequency.

The mechanism of this observed anomalous thermal transport is unexplained at present. However, we should note that the importance of thermal transports caused by ion acoustic waves has been recently pointed out.[13] The energy balance calculated at the skin layer requires the level of turbulence W/nT_e be of the order of 10^{-2} if the observed thermal transport is to be caused by ion acoustic waves. The energy transport by the waves is practically unhindered by the toroidal magnetic field in contrast to the conventional model[14] based on $\vec{E}\times\vec{B}$ random-walk processes and could play an important role in devices of high magnetic fields.

In conclusion, we have observed anomalously rapid thermal transport from a turbulent skin layer to the plasma core in a toroidal experiment. The speed of the energy transport is found to be

approximately 10^2 times faster than the classical value based on the anomalous collision frequency. Studies on the fluctuation level are underway.

The authors are grateful to Dr. K. Muraoka for useful discussions. Technical support by J. Ratzlaff and A. Witmans is appreciated. This research is sponsored by the National Research Council of Canada.

*On leave from the Department of Electrical Engineering, Utsunomiya University, Utsunomiya, Japan.

[1]R. D. Bengtson, K. W. Gentle, J. Jancarik, S. S. Medley, P. Nielsen, and P. Phillips, Phys. Fluids 18, 710 (1975).

[2]A. Hirose, T. Kawabe, and H. M. Skarsgard, Phys. Rev. Lett. 29, 1432 (1972).

[3]H. de Kluiver, private communication, and to be published.

[4]A. Hirose, H. W. Piekaar, and H. M. Skarsgard, to be published.

[5]L. E. Aranchuk, E. K. Zavoiskii, D. N. Lin, and L. I. Rudakov, Pis'ma Zh. Eksp. Teor. Fiz. 15, 33 (1972) [JETP Lett. 15, 22 (1972)].

[6]A. Hirose, Y. Amagishi, M. R. Shubaly, H. M. Skarsgard, and B. F. White, in *Proceedings of the Fifth International Conference on Plasma Physics and Controlled Nuclear Fusion Research, Tokyo, 1974* (International Atomic Energy Agency, Vienna, 1974), Vol. III, p. 299.

[7]S. Q. Mah, H. M. Skarsgard, and A. R. Strilchuk, Phys. Rev. Lett. 25, 1409 (1970).

[8]The cutoff density is 7×10^{13} cm^{-3}. The electron density 1×10^{14} cm^{-3} is obtained by extrapolating the density decay curve observed during the afterglow.

[9]The loop has a radius of 5.7 cm and is placed 17.2 cm beneath the midplane of the torus. The effective electric field (in V/cm) can be obtained from $E=1.785V_p - d(AI_p)/dt$, where V_p is the voltage observed on the oscilloscope [Fig. 4(a)], I_p is the plasma current (in amperes), and A, typically 2.5×10^{-9}, is determined by the plasma inductance and various mutual inductances. The time variation of the plasma inductance caused by the change of the skin-current profile is taken into account.

[10]R. H. Lovberg, in *Plasma Diagnostic Techniques*, edited by R. H. Huddlestone and S. L. Leonard (Academic, New York, 1965), Chap. 3.

[11]L. Spitzer, *Physics of Fully Ionized Gases* (Interscience, New York, 1962).

[12]R. A. Demirkhanov, A. G. Kirov, and M. Sh. Burdiashivili, Nucl. Fusion 11, 107 (1971).

[13]G. Pocobelli, A. Hirose, and I. Alexeff, Phys. Lett. 57A, 453 (1976).

[14]A. Hirose, K. E. Lonngren, and H. M. Skarsgard, Phys. Rev. Lett. 28, 270 (1972).

Theoretical Study of the Electronic Properties of Trigonal Se under Pressure

H. Wendel,* Richard M. Martin, and D. J. Chadi
Xerox Palo Alto Research Center, Palo Alto, California 94304
(Received 6 December 1976)

Pseudopotential calculations for the pressure dependence of the dielectric constants and energy-band structure of trigonal Se are presented. The calculations explain recent experimental observations of a strong pressure dependence for the optic spectra of Se. It is shown that interchain interactions and not local-field corrections are most important in describing the pressure data.

The pressure dependence of the optical properties of solids is determined by (i) changes in electronic states as a function of the spacings between atoms and (ii) explicit density dependence of the dielectric response function, for example, local-field effects.[1] Of particular interest in this respect are molecularlike solids in which the density can be increased greatly with pressure. Recently measurements of the reflectivity spectrum of trigonal Se under pressure have been reported by Kastner and Forberg (KF).[2] They interpreted their results in a molecular model, i.e., they completely neglected (i), and concluded that the large pressure-induced changes could be explained only by local-field effects included in (ii). In this Letter, we examine the electronic bands of Se under pressure and we show that the resulting optical properties, calculated with no local-field corrections, explain the results of KF. We find that the large effects observed by KF are, in fact, precursors of the transition of Se to a metallic nonmolecular structure, which occurs at 130 kbar.[3] We further argue why one expects a band picture for the electronic states to be adequate and local-field corrections to be small in Se.

Trigonal Se is a chainlike crystal, in which each atom is strongly bound to two nearest neighbors to form helical chains. The chains are packed together in a hexagonal pattern with each atom having weaker interactions with four more-